

BIAXIAL BEHAVIOUR OF THIN CONCRETE WALLS WITH ROCKING BASE CONNECTIONS

(Date received: 6.11.2006)

Nor Hayati binti Abdul Hamid¹ and Lionel Linayage²

¹Lecturer, Universiti Teknologi MARA, 40450 UiTM, Shah Alam, Selangor

²Postgraduate, Department of Civil Engineering, University of Canterbury, Christchurch, New Zealand

Email: abdulhamid_nrhyf@yahoo.com

ABSTRACT

Monolithic fixed-based wall panel experienced moderate/severe damage during ground motion. Thus, an alternative wall such as rocking wall system will provide safer structures with minimal damage. This paper will focus on the theoretical aspects resistance capacity followed by experimental works together with visual observation. Slender wall with slenderness ratio of 60:1 is tested under biaxial loading (in-plane and out-of-plane simultaneously) with different amplitudes and frequencies. The wall is constructed with steel-armoured at bottom of wall and a couple of flexural bending energy dissipator is used to absorb some energy during rocking mechanisms. Two-leaves clothes pattern with displacement control are applied to slender wall and some correlation between load and displacement are obtained. The hysteretic loops for in-plane and out-of-plane are plotted separately so that the seismic performance of rocking base connections can be analyzed and assessed accordingly. Finally, conclusion and recommendations are proposed for the construction of single storey warehouse buildings ranging from low to high seismic regions using spectral demands.

Keywords: Flexural Bending Energy Dissipator, Rocking Wall, Spectral Demand, Slender Wall, Steel-Armoured

1. INTRODUCTION

Rocking wall is an alternative wall panel to conventional fixed-base monolithic concrete wall which is designed specially for seismic regions. The strip foundation is clamped to rocking wall using unbonded post-tensioned tendons. The tendons are located at the centre of wall and remain elastic during rocking due to long unbonded length. The elastic restoring force in tendon acts as the primary lateral load resistance and eliminates any residual lateral displacement. Since the tendons are not bonded to the concrete, cracking of the concrete is minimal as the wall can be designed to remain elastic. Special detailing at base of the wall and reinforcement arrangement in rocking region at toe of the wall is necessary to eliminate any crushing and spalling of the concrete.

As the lateral load on the wall increases, the wall uplifts and non-linear lateral displacements occur due to the opening of a gap along the horizontal base. This results in bilinear elastic behaviour under lateral loads. The gap closes upon the removal of the lateral load and the wall re-centres. As the behaviour of such a system is bilinear elastic, it lacks any energy dissipation ability. Some energy is dissipated through radiation damping; however, for slender walls this is small. Therefore, supplemental mechanical energy dissipation devices may be incorporated into the walls in seismic areas where additional damping is needed.

Following a review of the state-of-the-art and an outline of the assessment of theoretical resistance of a rocking wall, details and results of an experiment carried out on a thin rocking wall under biaxial quasi-static loading is presented. Some design recommendations concerning biaxial response of slender precast concrete walls having rocking-base connections and recommendations for further research are also given.

2. LITERATURE REVIEW

The rocking structures under earthquake excitation are not a new phenomena, an earlier study was backdated by who defined the conceptual concepts of rigid rock body under ground motion. Meek [1] studied the aspects of structural flexibility coupled with rocking structures. Aslam *et al.* [2] investigated response rocking response of rigid bodies using vertical prestressed wires attach to the floor. Yim *et al.* [3] found that the response of rigid blocks is very sensitive to small changes in the sizes and slenderness ratio under horizontal and vertical ground motion. McManus *et al.* [4] and Priestley *et al.* [5] were investigated the seismic response of bridge structures which allowed them to rock freely on foundations beam. Psycharis and Jenning [6] suggested that the slender rigid bodies experience uplift while rocking depending on the connection between the base of structures and foundation beam.

The South Rangitikei Rail Bridge was the first structure followed by a rocking chimney at the Christchurch airport [7]. For framed buildings the idea of rocking connections was proposed by Priestley and Tao [8] to utilise unbonded prestressing in structures to provide lateral load resistance. Their intent was to provide unbonded prestressing tendons in beam-column connections in moment resisting frame structures and proposed an analytical method of designing such a connection. The clamping force provided by the prestressing force resists the shear demand in such a connection. This concept was later tested by Priestley and MacRae [9] and incorporated by Priestley *et al.* [10] in the PRESS 5-storey building designed, constructed and tested at the University of California at San Diego.

Mander and Cheng [11] proposed a new seismic design and construction methodology called "Damage Avoidance Design"

or DAD. In this approach the column longitudinal reinforcement is disconnected at the foundation beam-column interface. This allows the column to freely rock thus preventing low cycle fatigue and avoiding any damage to the concrete. Special reinforcement detailing for the rocking toe regions ensures that the structure behaves in a truly bilinear elastic manner without being damaged by seismic actions. Mander and Cheng [11] also developed an energy-based method to assess the equivalent viscous damping in rocking structures and a complete force deformation model for the rocking column accounting for structural flexibility (pre-rocking), rigid body kinematics (post-rocking) and prestressing action of the tendons. The theoretically predicted force-deformation behaviour was in good agreement with experimentally observed results for the quasi-static seismic performance of a near full size precast concrete rocking column bridge structure. This was further validated when Mander *et al.* [12] who undertook shaking table tests on a one-quarter-scale bridge model with rocking columns. In this case he took into account the effect of unbonded prestressing tendons, whether prestressed or slack. They also showed the effectiveness of the prestressed central tendons in reducing the lateral displacement of the rocking piers, thus increasing the structures seismic response.

Rahman and Restrepo [13] investigated quasi-static loading tests on 3 half-scale cantilever precast concrete rocking walls with identical reinforcement details except for the damping devices. One wall was without damping and others had identical damping devices incorporated at the wall base connection with simulated gravity loads by means of external prestressing on one of the two later walls. The wall panels were conventionally reinforced for satisfactory performance up to 2.5% design drift level. All the three walls performed well with only cosmetic damage at the rocking toe. High drift levels well in excess of 2.5% could be achieved with no residual drift upon unloading. Energy dissipators were effective and showed equivalent viscous damping ratios of up to 14%.

Holden *et al.* [14] continued their work by conducting an experimental study comparing the seismic performance of a monolithic emulation wall with a rocking wall. In the rocking wall, carbon fibre prestressing tendons and steel fibre reinforcement were incorporated along with supplemental yielding bar energy dissipators. The rocking wall reached a drift in excess of 6.0% with no visible damage to the wall prior to failure where as the emulative type wall failed at a drift of 2.5% due to fracture of the longitudinal reinforcement that was preceded by buckling. Moreover, in the case of rocking wall there was no residual drift upon unloading.

Toranzo [15] incorporated rocking connections in an experimental study on seismic performance of infilled frame and confined masonry construction. A three storey high wall model that incorporated steel flexural cantilever type mechanical energy dissipators was tested and confirmed that racking masonry walls provide an effective and damage-free alternative to damage-prone conventional fixed-base masonry shear wall as a primary lateral load system. The performance of cantilever type mechanical energy dissipators was also satisfactory.

Recently Sudarno and Mander [16] conducted research that was a companion study to the research presented herein on the performance of a thin precast concrete rocking wall under in-plane dynamic (shaking table earthquake) loading. Their rocking wall test specimen was identical to that of this study except for the concrete compressive strength. The performance of the wall was significantly better than that of its fixed-base monolithic emulation

counterparts. The wall returned to its original position without any discernable damage or residual displacements after a moderate level of earthquake excitation.

3. THEORETICAL RESISTANCE CAPACITY OF A SLENDER ROCKING WALL SYSTEM

In this section the in-plane and out-of-plane resistance of rocking walls are evaluated and a theoretical model for the prediction of rocking wall performance under biaxial lateral loading regime is presented.

3.1 IN-PLANE RESISTANCE OF ROCKING WALLS

A rocking wall which moves in-plane direction can be modelled using rigid body kinematics and strut-and-tie modelling. Figure 1 shows the external and internal forces acting on the wall while it is rocking. The wall height (H) and width (B) has an armoured rocking inter-face at the two rocking toe regions. The wall is armoured with a steel plate at the bottom and seated on a steel plate that is secured within the foundation. The uplift and rocking of wall under the application of a significant seismic force as shown in Figure 1(b) will activate energy dissipators and unbonded prestressing tendons. Thus, mobilised are the forces $(P_D)_1$, and $(P_D)_2$ in the energy dissipators located at eccentricities of ζ_1 , ζ_2 respectively from the centre of the wall, and P_p is the tendon prestress as shown in Figure 1(b). Tendon prestress is acting as clamping forces and gravity load from the wall (P_G) are designed to resist any sliding of the wall together with lateral loads representing seismic and/or wind actions. The summation of the dissipator forces is taken as P_D . The wall should also be designed to re-centre by the action of clamping and gravity forces upon the removal of lateral load. Figures 1(c) and (d) illustrate respective components of the resistance of energy dissipator, and gravity plus tendon prestress.

The lateral force F_{in} and drift angle θ_{in} are considered positive in the directions as shown in Figure 1(b), when the wall is rocking from left-to-right. The above properties are considered negative when the wall is rocking from right-to-left. The gravity, prestress and the dissipator forces, are always positive, as their effect is to clamp down the opening gap due to rocking. The eccentricity of the dissipator force is considered positive when it is measured from centre-line of the wall in the positive direction of the applied lateral force: thus the value of ζ_1 , is negative and the value of ζ_2 is positive.

For wall equilibrium, the disturbing moment about the rocking toe of the wall and the restoring moment are equated; thus for positive direction of rocking is given by:

$$F_{in}H = (P_G + P_p) \frac{B}{2} + P_{D1} \left(\frac{B}{2} - \zeta_1 \right) + P_{D2} \left(\frac{B}{2} - \zeta_2 \right) \quad \text{Equation (1a)}$$

Rearranging terms

$$F_{in}H = (P_G + P_p + P_D) \frac{B}{2} - (P_{D1}\zeta_1 + P_{D2}\zeta_2) \quad \text{Equation (1b)}$$

in which

$$P_D = P_{D1} + P_{D2} \quad \text{Equation (2)}$$

For negative direction of rocking

$$-F_{in}H = (P_G + P_p) \frac{B}{2} + P_{D1} \left(\frac{B}{2} + \zeta_1 \right) + P_{D2} \left(\frac{B}{2} + \zeta_2 \right) \quad \text{Equation (3a)}$$

Rearranging terms

$$-F_{in}H = (P_G + P_p + P_D) \frac{B}{2} + (P_{D1}\zeta_1 + P_{D2}\zeta_2) \quad \text{Equation (3b)}$$

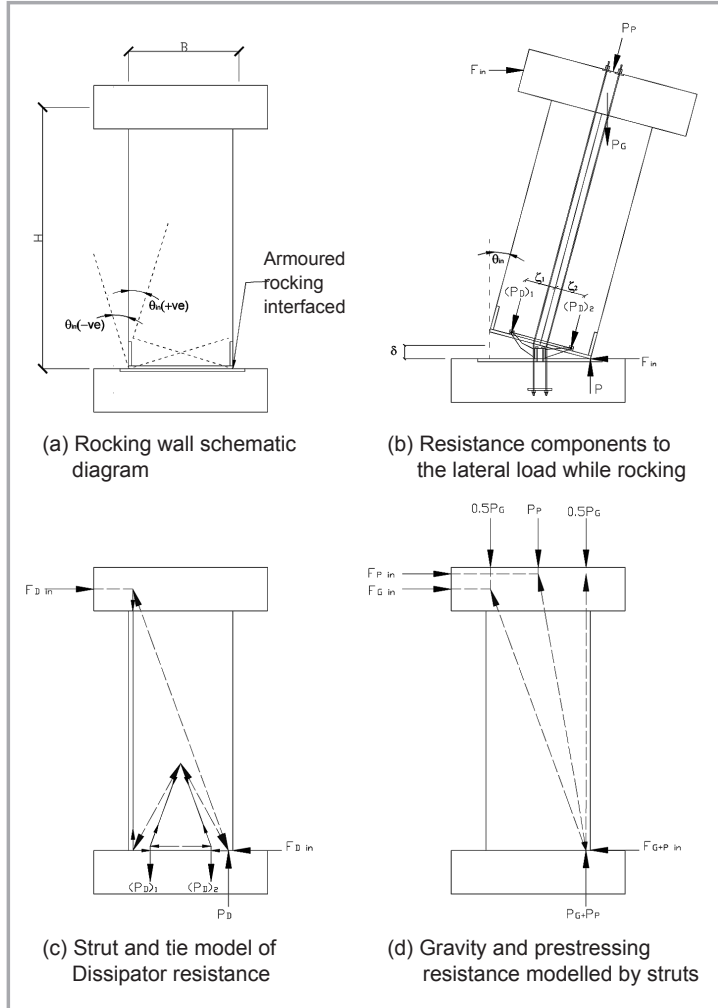


Figure 1: In-plane modelling of rocking wall

Equations (1b) and (3b) can be rewritten in a common form for both positive and negative directions of rocking and for any number of energy dissipators with their centroid acting at the centreline of the wall, as follows:

$$F_{in}H = \text{sgn}(\theta_{in})P \frac{B}{2} - \sum P_{Di}\zeta_i \quad \text{Equation (4)}$$

in which $\text{sgn}(\theta_{in})$ is +1 and -1 respectively for positive and negative directions of θ_{in} , and P total vertical force resistance. For vertical and horizontal equilibrium

$$P = P_G + P_p + P_D \quad \text{Equation (5)}$$

$$F_{in} = (F_G)_{in} + (F_p)_{in} + (F_D)_{in} \quad \text{Equation (5a)}$$

in which $(F_G)_{in}$, $(F_p)_{in}$, and $(F_D)_{in}$ are the equivalent lateral force resistances that can be balanced by the vertical resistances of gravity P_G , prestress P_p , and energy dissipator P_D respectively. The value of P_G is generally known from the wall and the building characteristics. The forces P_p and P_D ; hence F_p , F_D , are dependant on the lateral drift; that is the horizontal displacement at the top of the wall following uplift. This can be assessed based on rigid body kinematics, described in what follows.

The elongation of the prestressing tendons or strands is given by the central uplift of the wall δ , which can be expressed in terms of the wall drift angle θ_{in} and the wall width B ;

$$\delta = \theta_{in} \frac{B}{2} \quad \text{Equation (6)}$$

The tendons are designed to respond elastically during seismic events so that the wall restores its original position upon the removal of seismic action. Therefore, the change in tendon force can be expressed as,

$$\Delta P_p = \frac{\delta}{L_t} E_s A_p = \frac{1}{2} \theta_{in} \frac{B A_p E_s}{L_t} \quad \text{Equation (7)}$$

in which ΔP_p the change in prestress force; A_p and E_s respectively are the cross sectional area and the Young's modulus of prestressing tendon or strands; and L_t the length of prestressing tendons. The value of L_t is slightly greater than the wall height H , to include for the effect of anchorage zone. The value of P_p is the sum of the initial prestressing force P_i and the value of ΔP_p .

The response of the dissipators, however is not elastic, but its non linear response can conveniently be approximated as an elasto-plastic system as shown in Figure 2(a). Due to the Bauschinger effect of steel the actual dissipator response is somewhat different to a purely elasto-plastic system shown as shaded area. The dissipator resistance is added to the bilinear elastic response of the rocking wall with post-tensioned tendons as illustrated in Figure 2(b), where the shaded area corresponds to the dissipator effect. As an increasing lateral force is applied to the wall the system moves from point 0 to point 1, where the wall starts rocking. Subsequently at point 2, the arms of the energy dissipators yield simultaneously. A constant resistance of yielding dissipators is applied for further drift of the wall up to point 3, at which the system has reached the peak drift. The system then unloads via point 4 if the system were truly elasto-plastic, but due to the Bauschinger effects it directly goes from point 3 to point 5.

3.2 OUT-OF-PLANE RESISTANCE OF ROCKING WALLS

The out-of-plane response of the wall is not purely rocking but has both flexural and rocking response components. This is due to the nature of slender wall in which it first responds in a flexural manner until the lateral load is great enough to cause uplift in out-of-plane direction. The response of the wall subsequent to uplift both rocking and flexural; therefore both components should be taken into account for predicting out-of-plane response. These two components are treated separately as described in what follows.

The wall rocks in out-of-plane direction can be modelled as rigid body kinematics with the effect of gravity force is significant. P - Δ effect due to roof gravity force component is higher than self weight of slender wall. The difference in P - Δ effect is considered when modelling by taking the gravity force due to external (roof) load;

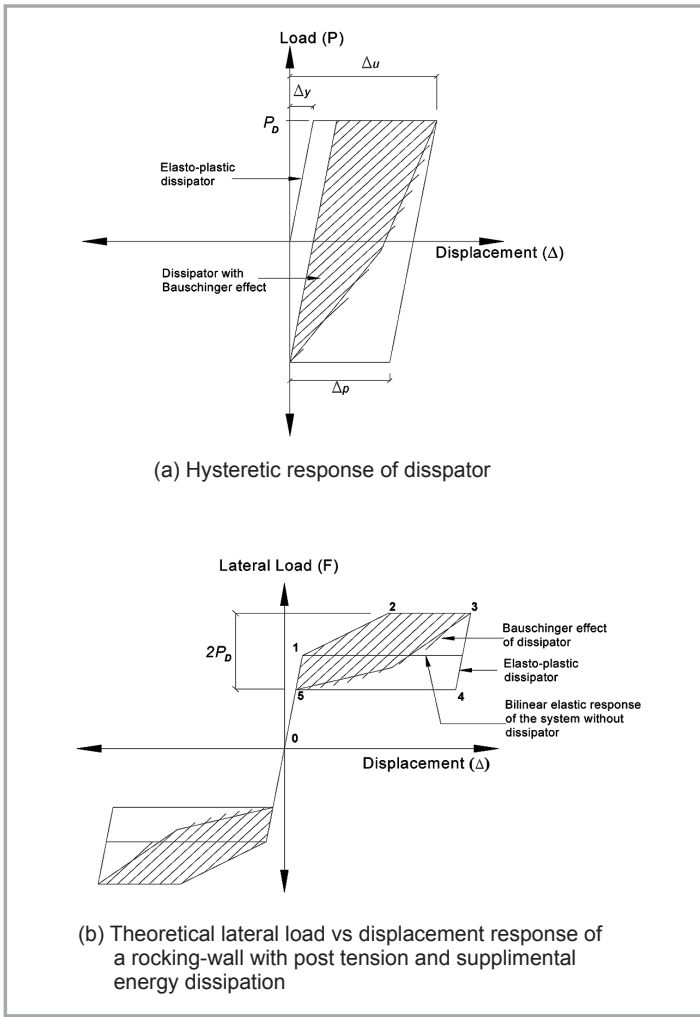


Figure 2 : Rocking behaviour of the wall with supplemental energy dissipation

(PG)E, acting at the top of the wall and the gravity force due to wall self weight; (PG)S, acting at mid height of the wall. The summation of the two components gives the total gravity force PG.

Figure 3 contrasts the schematic diagram of actions in out-of-plane direction for both positive and negative drifts. The out-of-plane lateral force F_{out} is considered positive in the direction as shown in Figure 3(a) and (b). For both positive and negative drift cases the equilibrium equation can be written as;

$$F_{out} = \text{sgn}(\theta_{out}) \left(\frac{P}{2} \left(\frac{t}{H} \right) - \left((P_G)_E + \frac{(P_G)_S}{2} \right) \theta_{out} \right) \quad \text{Equation (8)}$$

in which P is the total axial force given in equation (5a) and $\text{sgn}(\theta_{out})$ is +1 for positive drift angles of θ_{out} and is -1 for negative drift angles of θ_{out} .

Equation (8) holds true for an uncracked wall that behaves in a pure rocking manner. Nonetheless, the slender wall behaviour initially is flexural until uplift and is both flexural and rocking after uplift as illustrated in Figure 3(c) and (d). For initial flexural behaviour of slender wall is given by:

$$F_{out} = \frac{3EI_g}{H^3} \Delta_{out} = \frac{3EI_g}{H^2} \theta_{out} \quad \text{Equation (9)}$$

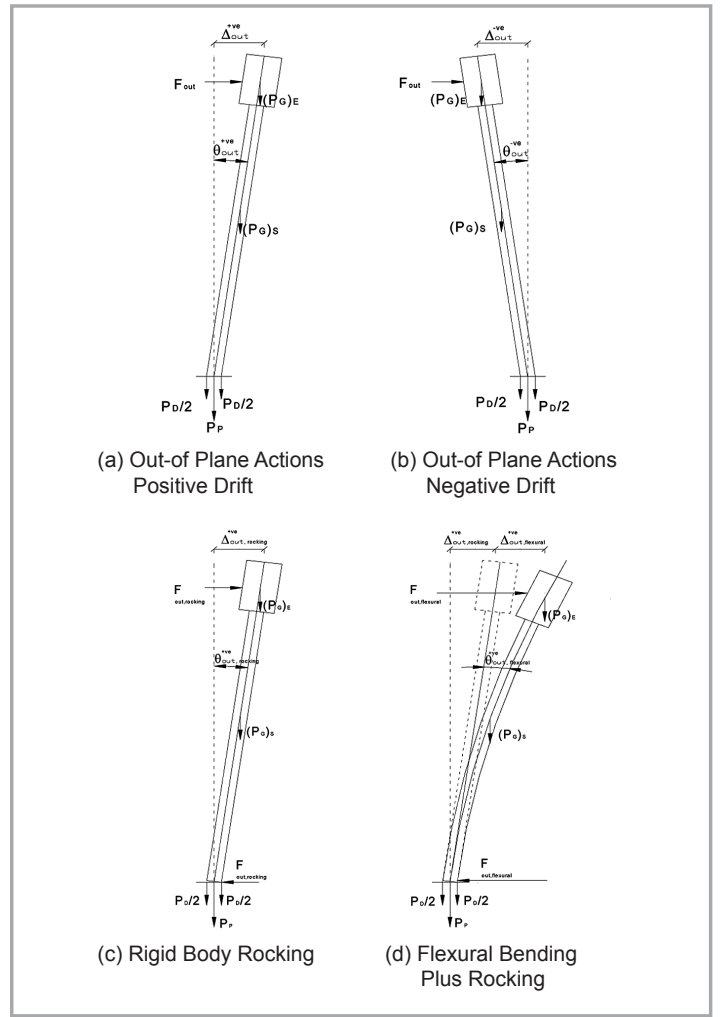


Figure 3: Schematic diagram of out-of-plane actions

If out-of-plane lateral force and out-of-plane drift with initial rocking are F_{out}^* and θ_{out}^* respectively, then Equation (9) becomes

$$F_{out}^* = \frac{3EI_g}{H^2} \theta_{out}^* \quad \text{Equation (10)}$$

But for equilibrium of the wall,

$$F_{out}^* = \frac{P}{2} \frac{t}{H} - \left((P_G)_E + \frac{(P_G)_S}{2} \right) \theta_{out}^* \quad \text{Equation (11)}$$

By substituting for F_{out}^* from Equation (10) in Equation (11) and rearranging the terms,

$$\theta_{out}^* = \frac{\frac{P}{2} \frac{t}{H}}{\left(\frac{3EI_g}{H^2} + (P_G)_E + \frac{(P_G)_S}{2} \right)} \quad \text{Equation (12)}$$

The rocking component of the lateral load can be found by the following expression.

$$F_{out,rocking} = \text{Sgn}(\theta_{out}) \left(\frac{P}{2} \frac{t}{H} - \left((P_G)_E + \frac{(P_G)_S}{2} \right) \alpha (\theta_{out} - \theta_{out}^*) \right) \quad \text{Equation (13)}$$

$$\theta_{out,rocking} = \alpha (\theta_{out} - \theta_{out}^*) \quad \text{Equation (14)}$$

and

$$\alpha = 1 - \frac{\theta_{out}^*}{\theta_{out}} \quad \text{Equation (15)}$$

The flexural component of the lateral load of the wall can be given by the following expressions. For the uncracked wall

$$F_{out, flexural} = \frac{3EI_g}{H^2} (1 - \alpha)(\theta_{out} - \theta_{out}^*) \quad \text{Equation (16)}$$

For the cracked wall

$$F_{out, flexural} = \frac{3EI_{eff}}{H^2} (1 - \alpha)(\theta_{out} - \theta_{out}^*) \quad \text{Equation (16)}$$

The cracking of the wall occurs when

$$f_t = \frac{P}{A_g} - \frac{M_{out, flexure}}{S_x} \quad \text{Equation (18)}$$

in which f_t tensile strength of concrete; P total axial force; A_g , gross area of wall; S_x , section modulus with respect to minor principal axis of wall; and $M_{out, flexural}$ out-of-plane moment given by

$$M_{out, flexural} = F_{out, flexural} H.$$

When simultaneous biaxial loading occurs the above expressions for in-plane and out-of-plane rocking are interdependent due to the biaxial interaction. However, the effect of out-of-plane drift has on in-plane behaviour is negligible as the tendon and dissipator forces are not greatly affected. The out-of-plane response on the other hand is dependant on the in-plane drifts and is accounted for in Equation (8) by the axial force P , which is composed of tendon and dissipator forces which are in-plane drift dependant. The theoretical force-displacement responses in both in-plane and out-of-plane directions can be established using Equation (4) through to Equation (18) and the theoretical force-displacement response of the energy dissipaters. The theoretical monotonic bilinear elastic in-plane and out-of-plane responses thus obtained for the range of in-plane and out-of-plane drift combinations used in this experiment are plotted with experimental results (the continuous gray lines) in Figures 9 (c) and (b) respectively.

4.0 DAMPING BEHAVIOUR OF ROCKING WALL SYSTEM

The energy enclosed within the shaded loop of the rocking-wall system response; Figure 2(b), provides the hysteretic damping, which is more frequently treated as equivalent viscous damping. The total effective viscous damping of the system is given by the summation of :

$$\xi_{eff} = \xi_{int\ rinsic} + \xi_{rocking} + \xi_{hysteretic} \quad \text{Equation (9)}$$

in which $\xi_{int\ rinsic}$ the damping due to internal actions within the system, the radiation damping due to the energy released during each rocking cycle, and the damping due to the energy dissipators.

Mander and Cheng [11] suggested an energy approach to assess the effective viscous damping factor of a rocking pier system. The same approach can be adopted here to deal with radiation (rocking) and hysteretic damping as follows;

$$\xi_{eq} = \frac{\delta E}{2\pi F_{max} \Delta_{max}} = \frac{\delta E}{2\pi C_c^{max} W_x \Delta_{max}} \quad \text{Equation (10)}$$

in which δE is the energy released per complete full cycle; Δ_{max} and F_{max} respectively are the maximum displacement and lateral force; W_x the inertial load; and C_c^{max} the base shear capacity

$$(C_c^{max} = \frac{F_{max}}{W_x}).$$

5. DESIGN OF ROCKING WALL PROTOTYPE

The design process begins with the assessment of structural period (T) of the system using the well-known relationship:

$$T = 2\pi \sqrt{\frac{m}{K}} \quad \text{Equation (11)}$$

where m is the mass ($m = W/g$) and K is the stiffness, which by definition for any nonlinear system is given by $K = F/\Delta$. After substituting for m and K in the expression of equation (11) and introducing the normalised base shear capacity C_c ; which is defined as $C_c = F/W$, give:

$$T = \sqrt{\frac{\Delta}{g C_c}} \quad \text{Equation (12)}$$

Figure 4 shows the moderate and long period of structures, the spectral base shear demand, $C_{D}(\xi_{eff})$ for any level of effective viscous damping is given as follows:

$$C_{D}(\xi_{eff}) = \frac{SA}{TB_L} \quad \text{Equation (13)}$$

where S the soil amplification factor; A the peak ground acceleration; T the secant period; and B_L a factor accounting for a damping level above the usual 5% damping which Pekcan *et al.* [17] have defined as

$$B_L = \left(\frac{\xi_{eff}}{0.05} \right)^{0.3} \quad \text{Equation (14)}$$

For the structural performance point the base shear demand is equal to the capacity ($C_c = C_D$), as shown in Figure 4(b), therefore by setting $C_c = C_D$ and substituting for T from Equation (12) into Equation (13) get:

$$C_c \Delta_{max} = \frac{g}{4\pi^2} \left(\frac{SA}{B_L} \right)^2 \quad \text{Equation (15)}$$

The product $C_c \Delta_{max}$ is the required seismic capacity in terms of the seismic demand, this can thus be determined from the right hand side of the expression based on an initial estimate of damping (and hence B_L). Further expanding of the left hand side of Equation (15) is possible as follows.

$$C_c = \frac{F}{W} = \frac{P}{W} \left(\frac{B}{2H} \right) \quad \text{Equation (16)}$$

By expanding P in Equation (16) as $P = P_G + P_P + P_D$, and knowing that maximum drift $\theta = \frac{\Delta_{max}}{H}$, Equation 15 is rewritten as:

$$\left(\frac{P_G + P_P + P_D}{W} \right) = \frac{g}{2\pi^2} \frac{1}{B\theta} \left(\frac{SA}{B_L} \right)^2 \quad \text{Equation (17)}$$

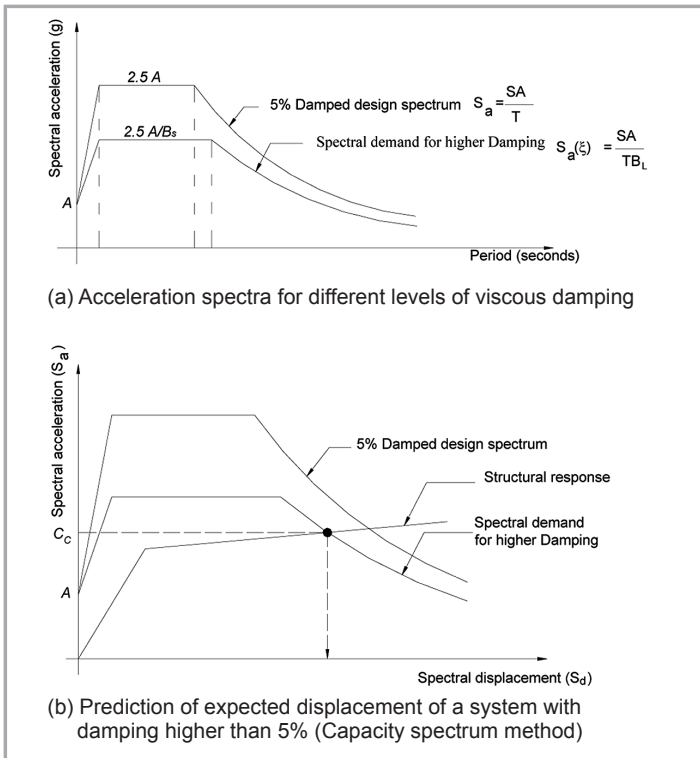


Figure 4: Spectral demands for systems with different viscous damping

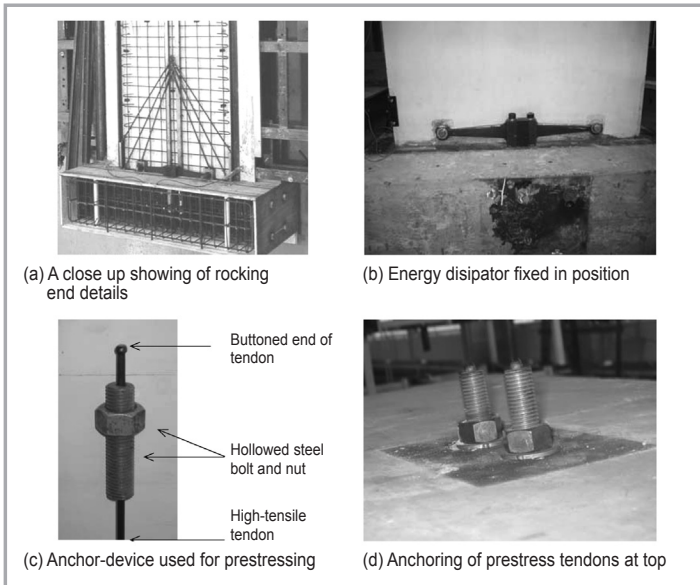


Figure 5: Details of rocking wall specimens

Table 1: Calculation of resistance capacity of the prototype rocking-wall

	SCENARIO-1 (MAXIMUM DRIFT = 3%, PGA = 0.8G)	SCENARIO-2 (MAXIMUM DRIFT = 2%, PGA = 0.4G)
ξ_{eff}	$0.025 + 0.005 + 0.07 = 0.10$	$0.025 + 0.005 + 0.05 = 0.08$
B_L	$\left(\frac{0.10}{0.05}\right)^{0.3} = 1.23$	$\left(\frac{0.08}{0.05}\right)^{0.3} = 1.15$
P/W	$\frac{g}{2\pi^2} \frac{1}{2.4 \times 0.03} \left(\frac{0.8}{1.23}\right)^2 = 1.23$	$\frac{g}{2\pi^2} \frac{1}{2.4 \times 0.02} \left(\frac{0.4}{1.15}\right)^2 = 1.25$
$P = P_G + P_P + P_D$	$2.92W = 808.84$	$1.25W = 346.25$
$P_P + P_D$	692 kN	229 kN

Therefore, by choosing an allowable maximum drift level for certain peak ground acceleration, the required overall resistance capacity of the wall can be determined. Two scenarios were considered in the case of the prototype wall design; in the first case a 3% maximum drift was allowed for a peak ground acceleration of 0.8g and in the second case a 2% maximum drift was allowed for a peak ground acceleration of 0.4g. For the damping values were assumed as $\xi_{intrinsic} = 2.5\%$, $\xi_{rocking} = 0.5\%$, for both cases and $\xi_{hysteretic} = 7\%$ and 5% for 3% and 2% drift respectively. The calculations are tabulated in Table 1. From the numerical calculation it is clear that Scenario-1 with 3% maximum allowable drift for 0.8g PGA governs the required capacity in the design of prototype wall.

5. EXPERIMENTAL STUDY

The test specimen was a 3/8th scale replica of the prototype and its combined prestress and dissipator capacity; when scaled down from the prototype of 692 kN, is 97 kN for a drift of 3%. Two prestressing tendons of 7mm diameter and four steel flexural cantilever type energy dissipators were used to provide the combined capacity of 97kN. The steel flexural cantilever type of energy dissipators had been previously installed and tested with satisfactory results on masonry rocking walls by Toranzo *et al.* [15]. This class of dissipator installed from outside of the structure is advantageous as the dissipators are expected to yield potentially necessitating replacement after a damaging earthquake attack, though the structure might not have experienced any damage.

Initial prestress was kept nearly at one third of the tendon yield stress giving a total initial prestress force of 30 kN; that is 15 kN in each of the two tendons. The energy dissipators were designed for 7.5 kN capacity to give a total dissipator force of 30 kN and the dissipator profile was chosen such that its arm yields throughout its length simultaneously when it reached its allowed capacity. This combination of prestressing tendons and energy dissipators give a slightly higher axial capacity of 116 kN than the required capacity of 97 kN at 3% drift.

6. CONSTRUCTION OF ROCKING SLENDER WALL

The important features of the rocking-end are: (a) discontinuation of longitudinal reinforcement at the base-joint of the wall, (b) provision of unbonded prestressing tendons, and (c) provision of energy dissipating dampers. The details are illustrated in Figure 5. The longitudinal reinforcement was cut-off at the joint and fillet-welded to a heavy steel plate provided at the bottom of the wall.

Prestressing tendons consisting of two 7 mm diameter high tensile steel wires were laid inside rectangular steel ducts and anchored inside the rocking base block at the bottom. The rectangular ducts were chosen as the circular ducts of sufficient internal diameter could not be accommodated within the limited thickness of the wall. Top ends of the tendons were anchored to the gravity blocks from top after post-tensioning each tendon up to 15 kN. The flexural mechanical energy dissipators of beam type were mounted at the base of the wall and ends of the energy dissipators were welded to heavy steel plates provided in the wall [Figure 5(a)].

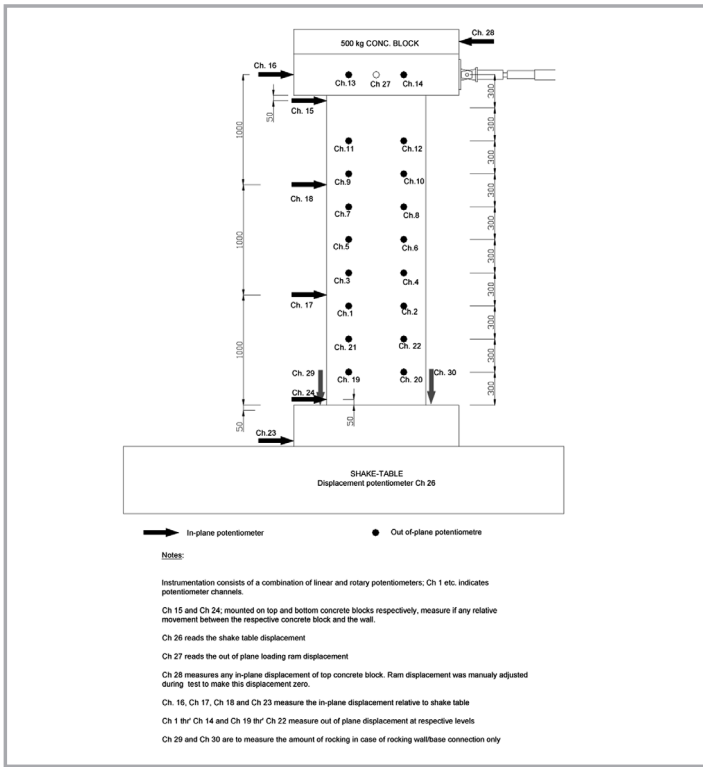


Figure 6: Experimental set-up and instrumentation for rocking slender wall

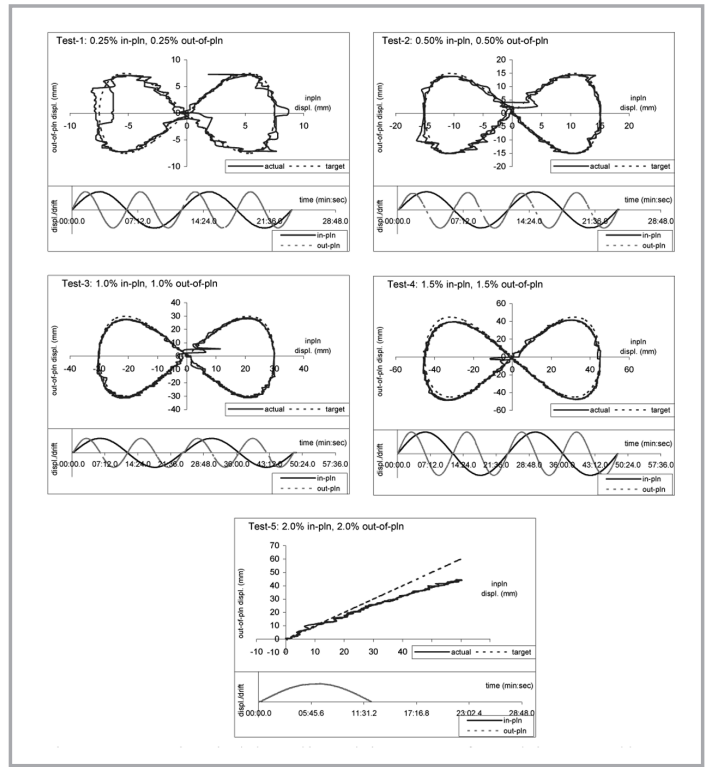


Figure 7: Biaxial loading history of rocking wall specimen.

6.1 TESTING OF THE SPECIMEN

Figure 6 shows the experimental setup and instrumentation of the specimen on shaking table. Linear potentiometers are used to measure vertical displacements of the ends wall and the strain gauges installed at each ends of the prestress tendons to measure strains. Quasi-static biaxial lateral loading pattern beginning from 0.25% drift amplitude cycles in both in-plane and out-of-plane directions to 1.5% drift amplitude cycles. The maximum value of 2.0% drift amplitude cycle was used with different to other cycles as its frequency in both orthogonal lateral directions were made equal. Figure 7 shows biaxial loading envelopes for slender wall and Table 2 shows the characteristics of the biaxial loading cycles.

7. EXPERIMENTAL RESULTS

The rocking wall specimen was tested up to 2% drift but not up to failure because it was a double-ended specimen, which was needed to be preserved for a second fixed-base wall experiment. The performance of the wall under biaxial quasi-static lateral loading was excellent with only cosmetic hairline cracks appearing at all levels of drifts to which the wall was subjected. Because of high slenderness, the out-of-plane response was dominated by flexure, hence the cracks generally oriented in horizontal direction.

However, the compression struts and the tension ties mobilised in the lower part of the wall by in-plane rocking caused cracks in the lower 500 mm of the wall to some extent deviate from horizontal direction. Slight deterioration of concrete could be observed near the ends of the vertical steel armour plate above the rocking toes and minor vertical cracking near energy dissipator points and prestress tendon ducts. Visual observation during testing is presented in Figure 8. It is apparent from the performance of the wall that the out-of-plane twisting at the base of the wall was prevented by the resistance of energy dissipators and the tendons prestress even though they were not specifically designed for this purpose.

The cyclic response of the wall during 1.5% drift amplitude cycle and 2.0% drift amplitude half-cycle are given Figure 9 and 10. It is noted herein however that the wall did not in reality experience 2.0 % drift level in the out-of-plane direction instead the drift was limited to 1.5% in that direction. The performance of the wall was significantly better than the walls with monolithic emulation connections. The maximum out-of-plane buckling at all levels of drift was within 6 mm or 13% of wall thickness. The out-of-plane twisting at the base was insignificant while that at the top of the wall was also very small compared to those of its monolithic emulation counterparts. More importantly the wall re-centred upon

Table 2: Characteristics of biaxial drift cycles of rocking-wall

Test	NUMBER DRIFT CYCLES		DRIFT%		FREQUENCY & (PERIOD)		
	E-W	N-S	E-W	N-S	E-W	N-S	
1	0.25%(E-W)/0.25%(N-S)	2	4	0.25	0.25	0.0014 Hz(720 sec)	0.0028 Hz(360 sec)
2	0.5%(E-W)/0.5%(N-S)	2	4	0.5	0.5	0.0014 Hz(720 sec)	0.0028 Hz(360 sec)
3	1.0%(E-W)/1.0%(N-S)	2	4	1.0	1.0	0.0007 Hz(1440 sec)	0.0014 Hz(720 sec)
4	1.5%(E-W)/1.5%(N-S)	2	4	1.5	1.5	0.0007 Hz(1440 sec)	0.0014 Hz(720 sec)
5	2.0%(E-W)/2.0%(N-S)	1/2	1/2	2.0	2.0	0.0007 Hz(1440 sec)	0.0007 Hz(1440 sec)

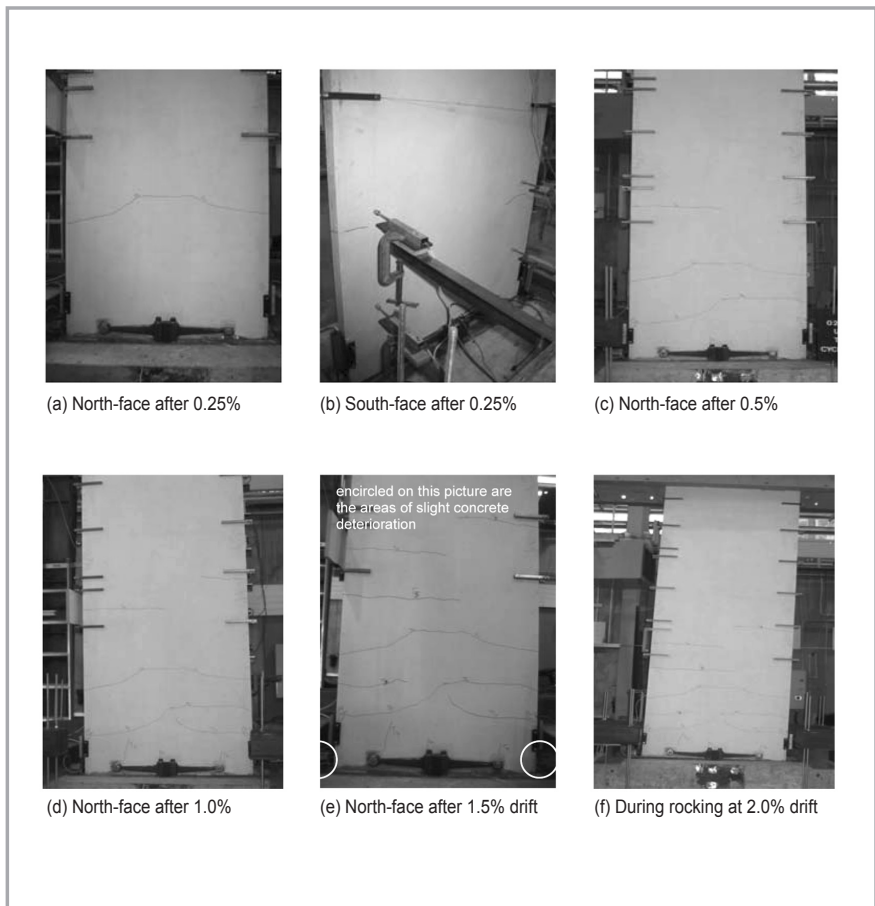


Figure 8: Visual observations during experiments on rocking wall

unloading after every level of drift and the residual displacement was within 3 mm even after 2.0% drift (Figure 12). It is interesting to note here that, it might be expected due to biaxial action, the tendon prestress was always higher than theoretically predicted for in-plane alone response and at 2.0% drift when tendon prestress achieved the design level at 3.0% in-plane drift.

Figure 11 shows the lateral load verses displacement response of the wall in both in-plane and out-of-plane directions. These are plotted together with the theoretically predicted response in the respective directions. The in-plane responses closely follow the predicted in-plane responses of within the investigated range of drift from 0.25% to 2.0% apparently with negligible effects of out-of-plane loading. Out-of-plane response is greatly affected by the in-plane drifts and does not follow clear hysteretic loops though it generally performs within the predicted bilinear elastic envelope except at 1.5% drift. The increasing axial load (compression) has a crack closing effect hence an enhanced stiffness of the cracked section than a constant axial load condition. This effect however diminishes later as can be seen in this case at 2% drift cycle. When it goes towards 2% drift the tendon prestress reaches its yield stress hence softening of the connection and a shortfall in out-of-plane resistance.

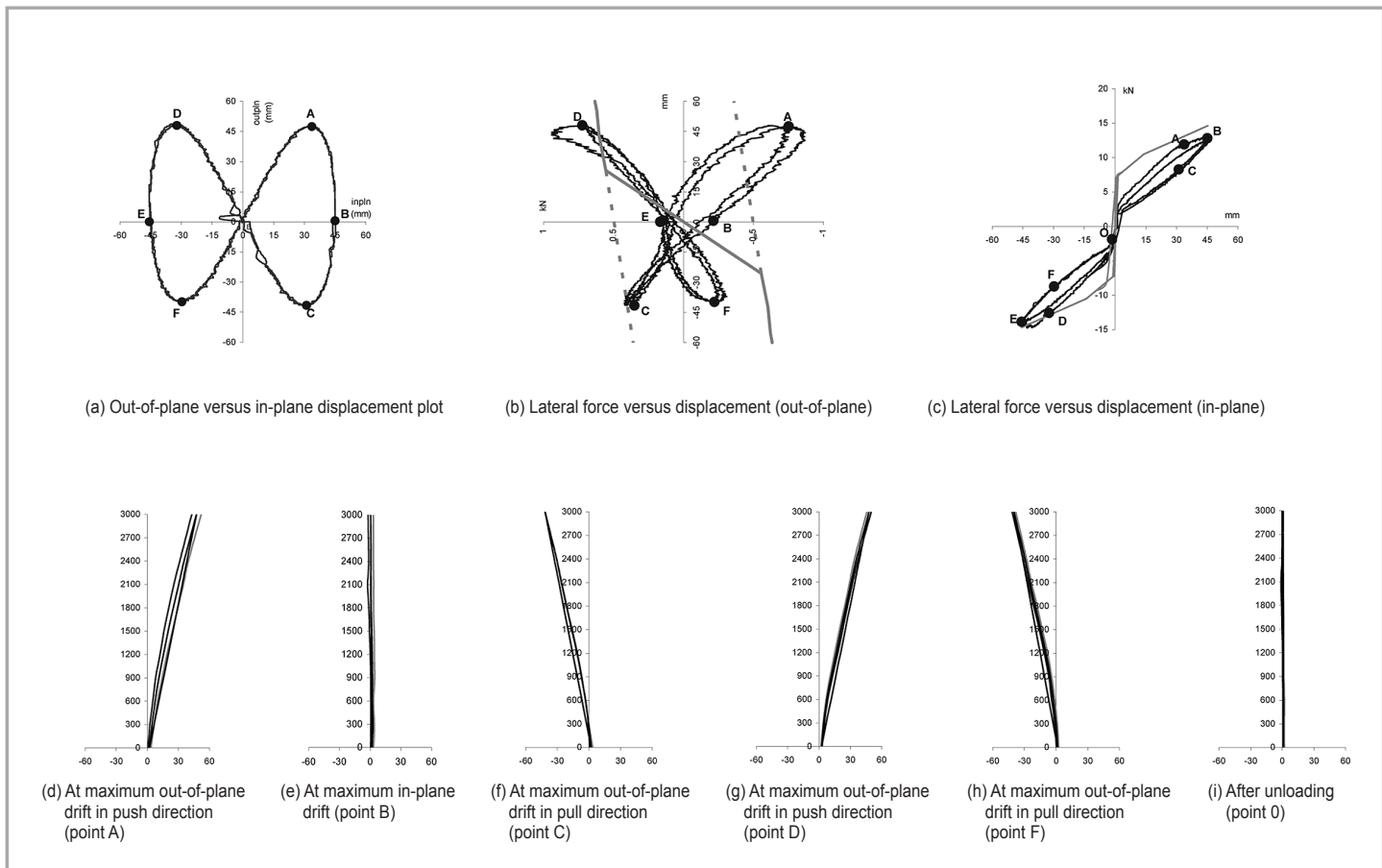


Figure 9: Cyclic response of rocking wall at 1.5% drifts cycle

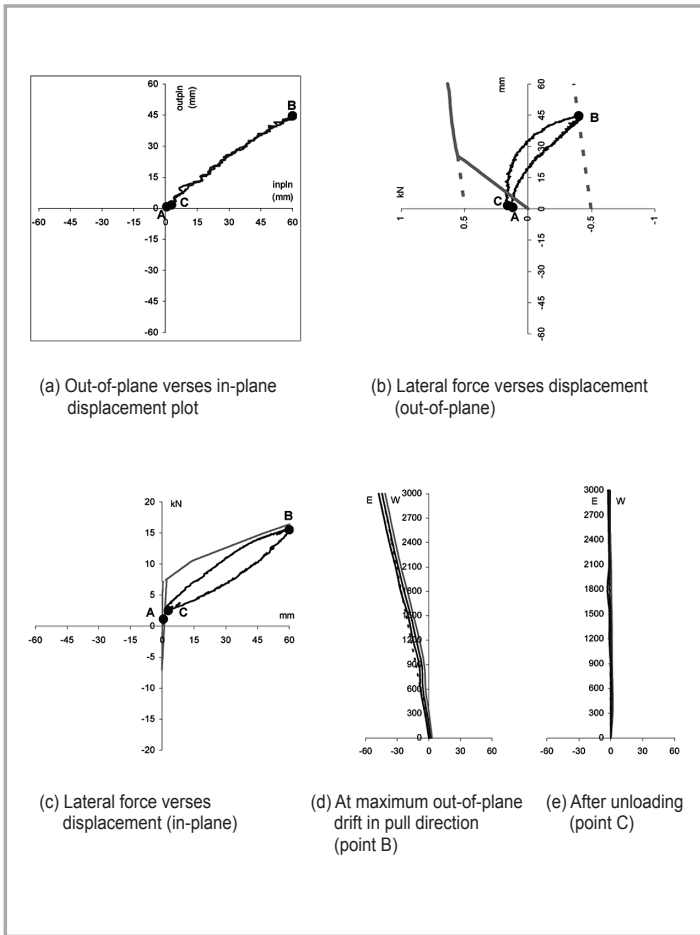


Figure 10: Cyclic response of rocking wall at 2% drifts half-cycle

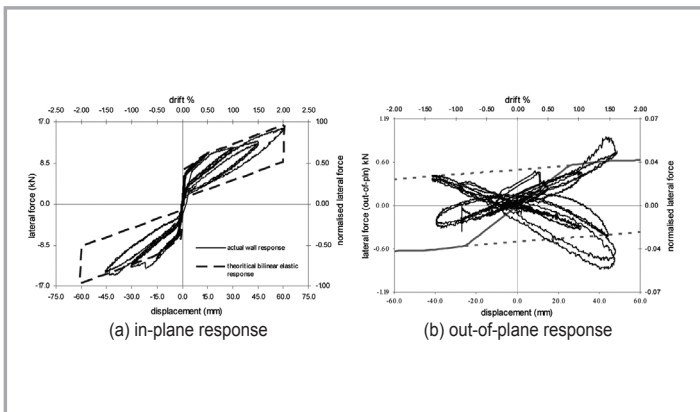


Figure 11: Hysteretic response of rocking wall

8.0 CONCLUSIONS AND RECOMMENDATION

Based on the research presented herein the following conclusions and recommendation are drawn for design and future investigation.

- a) The biaxial performance of the thin precast concrete rocking walls with slenderness of 60:1 was significantly better than the monolithic emulation base walls. The wall performed in an essentially bilinear elastic manner for the moderate levels of drift considered without showing any discernable damage while both of its fixed-base-emulation counterparts failed to survive that long.
- b) The out-of-plane buckling during and after the testing is very small and the wall re-centred upon unloading. Tendon prestress

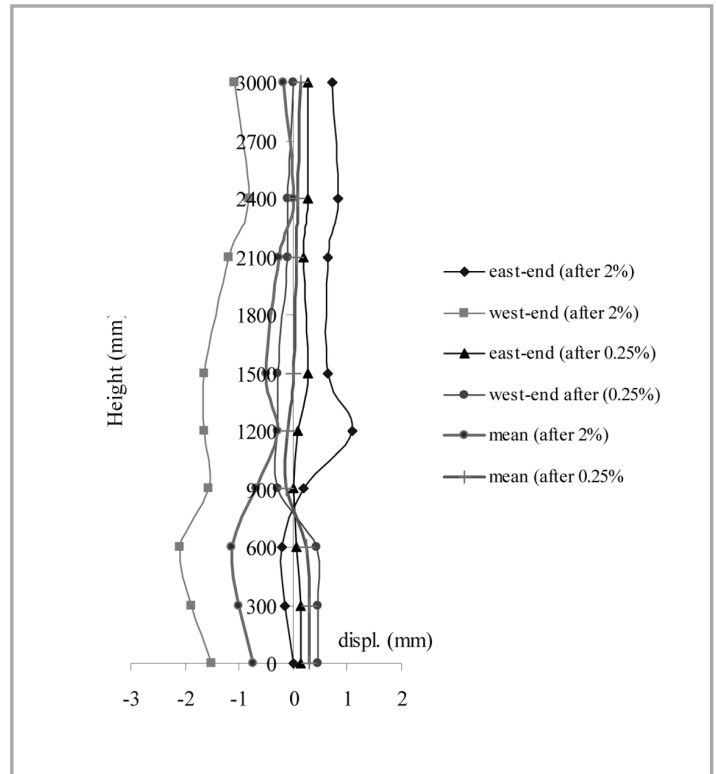


Figure 12: Hysteretic response of rocking wall

provided great resistance to out-of-plane deformations and brings the wall back to its original form during unloading. In-plane resistance of the wall is not significantly affected by the biaxial loading and closely follow the predicted in-plane alone response.

- c) The out-of-plane response was dominated by flexure, but did not follow a clear hysteretic pattern- this is due to cracking of the wall near its base.
- d) Thin precast concrete rocking walls can be designed for the in-plane alone loading, but if biaxial loading is likely to occur an increased tendon prestress capacity should be provided. For the likely loading of this type of structures, a 30% increase in prestress capacity should suffice.
- e) If biaxial lateral loading is likely occurred, wall cracking near the base of the walls, then for analysis and design $K=1$ (rather than $K = 0.7$ for in-plane loading alone).
- f) For reasons mentioned in the foregoing discussion the rocking wall specimen in this research was tested only up to a limited drift levels; 1.5% drift level in proper except for one (monotonic) half-cycle to a drift level of 2.0%, cycling was limited to $\pm 1.5\%$ drift. Therefore, it is desirable that additional experimental investigations on the out-of-plane behaviour and concurrent biaxial behaviour of thin precast concrete rocking walls at higher levels of drifts and variable (random) biaxial response be conducted. This is needed to study buckling and/or failure modes and to make any more definitive recommendations for analysis and design.
- g) It is likely that Euler Buckling may not be appropriate for thin rocking walls because of the initial high stiffness given by the prestress. A higher mode of Bifurcation Buckling after yielding of tendons may occur. This needs to be further investigated. Moreover, it is recommended that a more comprehensive lateral torsional buckling formulation be investigated. ■

REFERENCES

- [1] Meek, J.W. "Effects of Foundation Tipping on Dynamic Response", Journal Structural Division, ASCE, 101(7), pp 1297-1311, (1975)
- [2] Aslam, M., Goddon, W.G., and Scalise, D.T. (1980) "Earthquake Rocking Response of Rigid Bodies," Journal of Structural Engineering, ASCE, Vol.106, No.2, February 1980, pp 377-392.
- [3] Yim, C-S., Chopra, A.K. and Penzien, J. (1980). "Rocking Response of Rigid Blocks to Earthquake," Earthquake Engineering and Structural Dynamics, Vol. 8, pp565-587.
- [4] McManus, K.J., Priestley, M.J.N. and Carr, A.J. (1980)." The Seismic Response of Bridge Structures Free to Rock on their Foundations," Research Report No. 80/4, Department of Civil Engineering, University of Canterbury, Christchurch, New Zealand
- [5] Priestley, M.J.N., Evison, R.J., and Carr, A.J.(1978)." Seismic Response of Structures Free to Rock on Their Foundation," Bulletin of the New Zealand National Society For Earthquake Engineering , Vol. 20, No.3, September 1987, pp141-150.
- [6] Psycharis, I.N. and Jennings, P.C. (1983). "Rocking of Slender rigid Bodies allowed to Uplift," Earthquake Engineering and Structural Dynamics, Vol. 11, pp 57-76.
- [7] Skinner, R.I., Robinson, W.H. and McVerry, G.H., (1993), "An Introduction to Seismic Isolation", John Wiley & Sons.
- [8] Priestley, M.J.N., and Tao, J.T., (1993) "Seismic Response of Precast Prestressed Concrete Frames with Partially Debonded Tendons," PCI Journal, V. 38, No. 1, January-February 1993, pp 58-69
- [9] Priestley, M.J.N. and MacRae, G.A., (1996), "Seismic Testing of Precast Beam-to-Column Joint Assemblage with Unbonded Tendons," PCI Journal, Vol. 41, No. 1, pp. 64-80.
- [10] Priestley, M.J.N., Sritharan, S., Conley, J.R., Pampanin and S., (1999), "Preliminary Results and Conclusions From the PRESSS Five-Story Precast Concrete Test Building", PCI Journal, Vol. 44, No. 6, pp 42-67.
- [11] Mander, J.B., and Cheng, C-T., (1997). "Seismic Resistance of Bridge Piers Based on Damaged Avoidance Design," Technical Report NCEER-97-0014, NCEER, Department of Civil and Environmental Engineering, State University of New York at Buffalo.
- [12] Mander, J.B., Conteras, R. and Garcia, R., (1998), "Shaking Table Experiments on Bridge Piers with Rocking Columns," M.S. Report, State University of New York at Buffalo.
- [13] Rahman, A. and Restrepo, J.I., (2000). "Earthquake Resistant Precast Concrete Buildings: Seismic Performance of Cantilever Walls Prestressed Using Unbonded Tendons," Research Report, Department of Civil Engineering, University of Canterbury.
- [14] Holden, T.J., Restrepo, J.I., Mander and J.B.,(2001). "A Comparison of Seismic Performance of Precast Concrete Wall Construction: Emulation and Hybrid Approaches," Research Report 2001-4 Department of Civil Engineering, University of Canterbury.
- [15] Toranzo, L. A. (2004), Restrepo, JI., Carr, A.J. and Mander, J.B.(2004). "The Use of Rocking Walls in Confined Masonry Structures: A Performance-based Approach," 13th World Conference on Earthquake Engineering, Vancouver, B.C., Canada, August 1-6, 2004, Paper No.599.
- [16] Sudarno, I. and Mander, J.B, (2003). "Performance of Thin Precast Concrete Wall Panels under Dynamic Loading", ME Report, Department of Civil Engineering, University of Canterbury, Christchurch, New Zealand.
- [17] Pekcan, G., Mander, J.B. and Chen, S.S, "Fundamental Considerations for Design of Non-Linear Viscous Dampers", Earthquake Engineering and Structural Dynamics, 28, pp1405-1425.

PROFILE



ENGR. DR NOR HAYATI BINTI ABDUL HAMID

Engr. Dr Nor Hayati Abdul Hamid has been working as a lecturer at University Teknologi Mara, Shah Alam, Selangor for 16 years. She completed her PhD (Earthquake Engineering) from University of Canterbury, Christchurch, New Zealand in 2006. She received her Master of Science in Construction Management and Structural Engineering from University of NewCastle Upon Tyne, United Kingdom in 1993 and obtained her BSc (Civil Engineering) from University of Pittsburgh, United States of America in 1989. Her research interests are seismic performance of precast buildings under earthquake excitation, dynamic response of thin/slender wall, design of rocking precast hollow core walls under earthquake, cyclic behaviour of precast hollow core slabs and the interaction of beam-column joints under quasi-static reverse cyclic loading.

LIONEL LINAYAGE

Postgraduate, Department of Civil Engineering, University of Canterbury, Christchurch, New Zealand.